

## Characterization of Fas (Apo-1, CD95)-Fas Ligand Interaction\*

(Received for publication, April 16, 1997, and in revised form, May 9, 1997)

Pascal Schneider‡§, Jean-Luc Bodmer‡, Nils Holler‡, Chantal Mattmann‡, Patricia Scuderi‡, Alexey Terskikh‡, Manuel C. Peitsch¶, and Jürg Tschopp‡

From the ‡Institute of Biochemistry, University of Lausanne, BIL Biomedical Research Center, CH-1066 Epalinges, Switzerland and ¶Glaxo Institute for Molecular Biology, CH-1228 Plan-Les-Ouates, Switzerland

The death-inducing receptor Fas is activated when cross-linked by the type II membrane protein Fas ligand (FasL). When human soluble FasL (sFasL, containing the extracellular portion) was expressed in human embryo kidney 293 cells, the three *N*-linked glycans of each FasL monomer were found to be essential for efficient secretion. Based on the structure of the closely related lymphotoxin  $\alpha$ -tumor necrosis factor receptor I complex, a molecular model of the FasL homotrimer bound to three Fas molecules was generated using knowledge-based protein modeling methods. Point mutations of amino acid residues predicted to affect the receptor-ligand interaction were introduced at three sites. The F275L mutant, mimicking the loss of function murine *gld* mutation, exhibited a high propensity for aggregation and was unable to bind to Fas. Mutants P206R, P206D, and P206F displayed reduced cytotoxicity toward Fas-positive cells with a concomitant decrease in the binding affinity for the recombinant Fas-immunoglobulin Fc fusion proteins. Although the cytotoxic activity of mutant Y218D was unaltered, mutant Y218R was inactive, correlating with the prediction that Tyr-218 of FasL interacts with a cluster of three basic amino acid side chains of Fas. Interestingly, mutant Y218F could induce apoptosis in murine, but not human cells.

The Fas ligand (CD95 ligand) is a 40-kDa type II membrane protein belonging to the tumor necrosis factor (TNF)<sup>1</sup> family of proteins (1, 2). This family consists of trimeric ligands that induce defined cellular responses upon binding to their respective receptors. Fas and the other members of the TNF receptor family are type I membrane proteins. They are characterized by the presence of cysteine-rich motives conferring an elongated structure to their extracellular domains (1).

The Fas ligand is one of the major effectors of CD8<sup>+</sup> cytotoxic T lymphocytes (3, 4) and natural killer cells (5). It is also involved in the establishment of peripheral tolerance (6), in the

activation-induced cell death of lymphocytes (7–10), and in the delimitation of immunoprivileged regions such as the eye and testis (11, 12). Along the lines of this latter feature, cotransplantation of myoblasts engineered to express FasL can protect an islet allograft from rejection (13). The loss of function due to mutations in murine Fas ligand (*gld*), murine Fas (*lpr*), human Fas, or human FasL leads to lymphoproliferation, lymphadenopathy, and autoimmune diseases (14–18). Fas-null mice have a similar but more severe phenotype (19).

The Fas-FasL system is implicated in a number of pathogenesis. Abnormally elevated levels of soluble Fas ligand are detected in leukemia/lymphomas of T and natural killer cells, and in an aggressive nasal lymphoma (20, 21). Various tumor cells express FasL, therefore potentially creating their own immunoprivileged sites (22–24). The Fas/Fas ligand system is also involved in the CD4<sup>+</sup> T cell deletion observed in human immunodeficiency virus-infected individuals (25–27), in multiple sclerosis (28), and in acute graft-versus-host disease (29, 30).

Membrane-bound Fas ligand can be processed into a soluble form by a metalloprotease whose inhibitor profile is similar to that of the protease solubilizing TNF $\alpha$  (20, 31–34). The soluble forms of the TNF family members that have been crystallized so far include TNF $\alpha$  (35), lymphotoxin  $\alpha$  (also known as TNF $\beta$ ) (36), and CD40L (37). They all share a similar conformation resulting in a compact, pear-shaped trimeric structure. Other family members (Fas ligand (38), TRAIL (39), CD30L, CD27L, OX40L, and 4-1BBL) show clear sequence homology at the amino acid level, and there is little doubt that they are all trimeric.

In this study, we produce biologically active human soluble Fas ligand (sFasL) and amino acid residues essential for the Fas/FasL interaction are identified. We also demonstrate the importance of extensive *N*-glycosylation for the efficient secretion of FasL.

### EXPERIMENTAL PROCEDURES

#### Materials

The anti-flag M2 monoclonal antibody and the anti-flag M2 antibody coupled to agarose were purchased from Integra Biosciences (Wallisellen, Switzerland). Protein A-Sepharose was purchased from Pharmacia (Uppsala, Sweden). Tunicamycin and Protein A were obtained from Sigma (Buchs, Switzerland). Peptide *N*-glycanase F was purchased from New England Biolabs (Schwalbach, Germany). The PCR-2 TA cloning vector and PCR-3 mammalian expression vector were obtained from InvitroGen (NV Leek, the Netherlands). Cell culture media and antibiotics were obtained from Life Sciences (Basel, Switzerland). The non-radioactive cell proliferation assay was purchased from Promega (Wallisellen, Switzerland). The fusion protein muFas-Fc was kindly provided by Dr. C. A. Smith (Immunex, Seattle, WA).

#### Cells

Murine B lymphoma A20 cells were grown into DMEM containing 5% heat-inactivated fetal calf serum (FCS) and the human T lymphoblastoma Jurkat cell line was grown in RPMI supplemented with 10% FCS. Human embryonic kidney 293 cells (ATCC CRL 1573) were cultured in DMEM:nutrient mix F-12 (1:1) supplemented with 2% FCS.

\* This work was supported by grants from the Swiss Federal Office of Public Health and the Swiss National Science Foundation (to P. S. and J. T.). The costs of publication of this article were defrayed in part by the payment of page charges. This article must therefore be hereby marked "advertisement" in accordance with 18 U.S.C. Section 1734 solely to indicate this fact.

§ To whom correspondence should be addressed: Institut de Biochimie, Université de Lausanne, Ch. des Boveresses 155, CH-1066 Epalinges, Switzerland. Tel.: 41-21-692-5743; Fax: 41-21-692-5705; E-mail: pascal.schneider@ib.unil.ch.

<sup>1</sup> The abbreviations used are: TNF, tumor necrosis factor; sFasL, recombinant human soluble Fas ligand; DMEM, Dulbecco's modified Eagle's medium; FCS, fetal calf serum; PCR, polymerase chain reaction; hFas-Fc, human Fas-Fc; muFas-Fc, murine Fas-Fc; ELISA, enzyme-linked immunosorbent assay; PBS, phosphate-buffered saline; PAGE, polyacrylamide gel electrophoresis; MTS, 3-(4,5-dimethylthiazol-2-yl)-5-(3-carboxymethoxyphenyl)-2-(4-sulfophenyl)-2H-tetrazolium, inner salt.

Human embryonic kidney 293 cells stably transfected with the large T antigen of SV40 (293T cells, kindly provided by Dr. M. E. Peters, German Cancer Research Center, Heidelberg, Germany) were grown in DMEM supplemented with 10% FCS. All media contained antibiotics (penicillin and streptomycin at 5  $\mu\text{g/ml}$  each and neomycin at 10  $\mu\text{g/ml}$ ).

#### Expression Vectors for the Recombinant sFasL and the Soluble Human Fas-Human Immunoglobulin Fc Chimera

**sFasL**—A DNA fragment coding for the signal peptide of hemagglutinin, including 6 bases of its 5'-untranslated sequence (40), the flag epitope (41), a linker (GPGQVQLQ), and the *Pst*I, *Sal*I, *Xho*I, and *Bam*HI restriction sites, was cloned between the *Hind*III and *Bam*HI sites of a modified PCR-3 vector in which nucleotides 720–769 had been deleted. This plasmid was called pHAflag-038. The full-length cDNA of human Fas ligand was amplified by PCR from the cDNA of activated peripheral blood lymphocytes (oligonucleotides: 5'-CCTCTACAGGACT-GAGAAGAAG-3' and 5'-CAACATTCTCGGTGCCTGTAAC-3'), and cloned into PCR-2 TA cloning vector. This plasmid was used as PCR template for the amplification of a portion of the extracellular domain of the FasL (amino acids 139–281) with suitable restriction sites added at each end. The resulting *Pst*I/*Eco*RI fragment was inserted into pHAflag-038, in frame with the flag sequence.

For each point mutation, a set of complementary oligonucleotides containing the target mutation was used. In the first round of the PCR, two products were produced with pHAflag-FasL as template using: (a) the forward oligonucleotide and Sp6 primer, and (b) the reverse oligonucleotide and T7 primer. Purified PCR products, containing the 3' and 5' portions of FasL, respectively, were mixed and allowed to undergo three cycles of PCR before amplification with T7 and Sp6 primers. The *Pst*I/*Eco*RI fragment of the resulting PCR product was cloned into pHAflag-038.

**hFas-Fc**—The extracellular domain of hFas (GenBank X63717, nucleotides –24 to 510, the A of ATG being nucleotide 1) with 5' *Hind*III and 3' *Sma*I sites was amplified by PCR from a full-length cDNA clone (kindly provided by Prof. P. H. Krammer, German Cancer Research Center, Heidelberg). The *Hind*III-*Sma*I fragment was cloned between the *Hind*III and *Eco*RV sites of a modified PCR-III vector containing an added *Sal*I site after the existing *Eco*RV site. A *Sal*I/*Not*I cDNA cassette encoding the hinge, CH2, and CH3 domains (amino acid residues 231–447) of human IgG1 (42) was cloned in frame at the 3' end of the extracellular domain of Fas. Both strands of each construct were checked by sequencing.

#### Expression of sFasL and hFas-Fc

Plasmids were either expressed transiently in 293T cells or stably in 293 cells. Plasmids (10  $\mu\text{g}$ ) were transfected by the calcium phosphate method ( $3 \times 10^5$  cells/28-cm<sup>2</sup> plate) in HEPES buffer (43). After transfection, cells were grown for 48–72 h in serum-free Opti-MEM medium, and supernatants were harvested. Stably transfected 293 cells were obtained by selection in 800  $\mu\text{g/ml}$  G418 (70% active) for 2 weeks and cloned at that stage. Supernatants of stably transfected clones were harvested after 10–12 days in culture and screened by Western blotting or receptor binding ELISA (see below) for expression levels.

#### Peptide N-Glycanase F Digestion of sFasL

293 cells ( $2 \times 10^5$ ) transiently transfected with sFasL and their corresponding supernatants ( $20 \times$  concentrated, 15  $\mu\text{l}$ ) were heated in 20  $\mu\text{l}$  of 0.5% SDS, 1% 2-mercaptoethanol for 3 min at 95 °C. Samples were cooled and supplemented with 10% Nonidet P-40 (2  $\mu\text{l}$ ) and 0.5 M sodium phosphate, pH 7.5 (2  $\mu\text{l}$ ). Peptide N-glycanase F (125 units/ $\mu\text{l}$ , 1  $\mu\text{l}$ ) was added (or omitted in controls), and samples were incubated for 3 h at 37 °C prior to analysis by Western blotting.

#### Purification of sFasL and hFas-Fc

Supernatants of stably transfected cells were filtered using a 0.22- $\mu\text{m}$  membrane and loaded as 40-ml aliquots onto 1-ml columns of anti-flag M2 agarose (for sFasL) or Protein A-Sepharose (for hFas-Fc) equilibrated in PBS. The columns were washed with 10 ml of PBS and eluted with 2.5 ml of 50 mM citric acid. The eluate was neutralized with 1 M Tris base, concentrated, and exchanged into PBS using Centrprep-30 concentrators. Protein concentration was determined by the bicinchoninic acid method (Pierce) using bovine serum albumin as the standard, and the purity of the samples was assessed by SDS-PAGE and Coomassie Blue staining.

#### SDS-PAGE and Western Blotting

SDS-PAGE and Western blotting were performed on 12% mini gels according to previously published methods (44, 45). Blots were incubated with anti-flag M2 monoclonal antibodies (5  $\mu\text{g/ml}$ , 0.02% NaN<sub>3</sub>, in blocking buffer: PBS, 0.5% Tween 20, 4% skim milk), followed by rabbit anti-mouse immunoglobulins coupled to horseradish peroxidase (diluted 1:2000 in blocking buffer). Peroxidase activity was detected by enhanced chemiluminescence.

#### Inhibition of N-Glycosylation with Tunicamycin

Tunicamycin was stored at –70 °C at a concentration of 1 mg/ml in 10 mM Tris-HCl, pH 9. Stably transfected cells secreting sFasL were grown for 10 days in the presence of 1, 100, or 1000 ng/ml tunicamycin. Cells and supernatants were harvested and analyzed by Western blotting.

#### Cytotoxic Assay

A20 or Jurkat cells (100  $\mu\text{l}$ , 50,000 cells, in 96-well plates) were incubated at 37 °C in the presence of sFasL at the indicated concentrations and 1  $\mu\text{g/ml}$  M2 monoclonal antibody. In some experiments, hFas-Fc or muFas-Fc was added at the indicated concentrations in the presence of 1  $\mu\text{g/ml}$  Protein A. Four to 8 h after the addition of FasL, 20  $\mu\text{l}$  of a solution containing 2 mg/ml 3-(4,5-dimethylthiazol-2-yl)-5-(3-carboxymethoxyphenyl)-2-(4-sulphophenyl)-2H-tetrazolium, inner salt (MTS) reagent (Promega) and 50  $\mu\text{g/ml}$  phenazine methosulfate was added to the cells. Following color development (2–4 h), absorbance at 490 nm was taken with an ELISA reader.

#### In Vitro Fas-FasL Binding Assay

96-well ELISA plates (Nunc Maxisorp) were coated with either hFas-Fc or muFas-Fc (1  $\mu\text{g/ml}$  in PBS, 100  $\mu\text{l}$ , 2 h, 37 °C). The following incubation and washing steps were performed: (a) saturation in block buffer (PBS, 5% FCS, 300  $\mu\text{l}$ , 1 h, 37 °C), (b) three washes (PBS, 0.05% Tween-20), (c) incubation with sFasL (10–1000 ng/ml in PBS containing 50  $\mu\text{g/ml}$  bovine serum albumin, 100  $\mu\text{l}$ , 1 h, 37 °C), (d) three washes, (e) incubation with M2 monoclonal antibody (1  $\mu\text{g/ml}$  in block buffer, 100  $\mu\text{l}$ , 37 °C, 30 min), (f) three washes, (g) incubation with rabbit anti-mouse IgG coupled to peroxidase (1/1000 dilution in block buffer, 100  $\mu\text{l}$ , 30 min, 37 °C), (h) three washes, (i) detection (0.3 mg/ml o-phenylenediamine hydrochloride, 0.01% H<sub>2</sub>O<sub>2</sub> in 50 mM citric acid, 100 mM Na<sub>2</sub>HPO<sub>4</sub>, 200  $\mu\text{l}$ , as necessary (1–5 min), 25 °C), and (j) termination (2 N HCl, 50  $\mu\text{l}$ ). Absorbance was taken at 490 nm with an ELISA reader.

#### Gel Permeation Chromatography

sFasL samples (5  $\mu\text{g}$  in 100  $\mu\text{l}$ ) were mixed with the internal standards catalase and ovalbumin, then loaded onto a Superdex-200 HR10/30 column, and the proteins were eluted in PBS at 0.5 ml/min. Fractions (0.25 ml) were analyzed using the receptor binding ELISA (using 5  $\mu\text{l}$  of fractions for active ligands), and Western blotting was carried out after trichloroacetic acid precipitation of the entire fraction. The column was calibrated with standard proteins: thyroglobulin (669 kDa), ferritin (440 kDa), catalase (232 kDa), aldolase (158 kDa), bovine serum albumin (67 kDa), ovalbumin (43 kDa), chymotrypsinogen A (25 kDa), and ribonuclease A (13.7 kDa).

#### Protein Modeling

Molecular models for both Fas and FasL were generated using knowledge-based protein modeling methods as implemented in the Swiss-Model server (46, 47). A molecular model for FasL was built using the known tridimensional structures of both TNF $\alpha$  (48) and lymphotoxin  $\alpha$  (TNF $\beta$ ) (49) (Protein Data Bank entries 1TNF and 1TNR chains A, B, and C) (50). The known structure of the 55-kDa tumor necrosis factor receptor (51) was used to produce a molecular model for Fas. In both cases, the modeling procedure was started by submitting the respective protein sequences to Swiss-Model via the First Approach Mode. The resulting models were then used to correct the automated multiple sequence alignments generated by the server in several loop regions. These corrected alignments were resubmitted to Swiss-Model through the Optimize Mode. The resulting models were structurally sound, and did not show obvious sequence or structure inconsistencies (51) according to three-dimensional/one-dimensional profiles (52) and ProsaII (53). The quaternary structure of the Fas-FasL complex was generated using the x-ray structure of the human lymphotoxin  $\alpha$ -TNF receptor I complex (54). Three copies of the ligand model and three copies of the receptor model were superimposed onto the corresponding subunits of the experimental structure. The hexameric protein complex

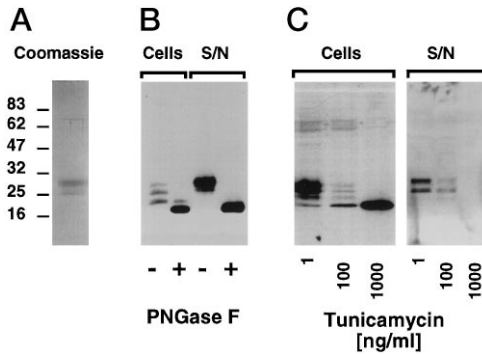


**FIG. 1. Glycosylation of sFasL.** Panel A, Coomassie Blue staining of sFasL. The flag-tagged sFasL in conditioned supernatants of stably transfected 293 cells was affinity-purified on anti-flag M2 agarose, and 1.5  $\mu$ g was analyzed by SDS-PAGE (12%) followed by Coomassie Blue staining. The molecular mass markers (in kDa) are indicated. Panel B, peptide *N*-glycanase F digestion of sFasL. 293 cells transiently transfected with flag-tagged sFasL were grown for 72 h in serum-free medium. Cell extracts (Cells,  $2.5 \times 10^5$  cells/lane) and  $20 \times$  concentrated supernatant (S/N, 15  $\mu$ l/lane) were treated with or without peptide *N*-glycanase F (PNGase F) and analyzed by Western blotting using anti-flag M2 antibodies. Panel C, the effect of tunicamycin on the glycosylation and secretion of sFasL. Stably transfected 293 cells were grown for 10 days in serum-free medium and in the presence of the indicated concentrations of tunicamycin. Cells ( $2.5 \times 10^5$ /lane) and supernatants (20  $\mu$ l) were analyzed by Western blotting using anti-flag M2 antibodies.

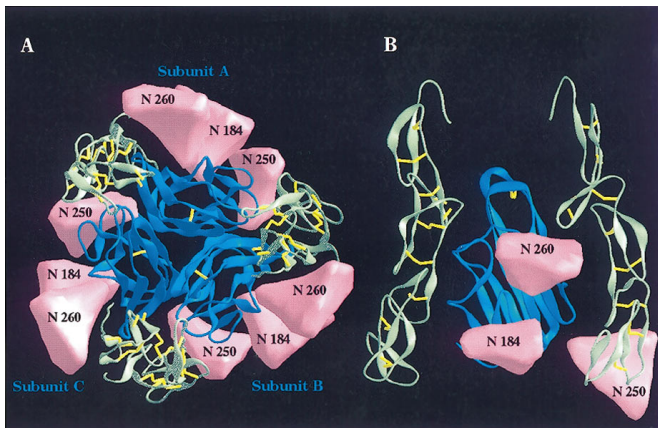


**FIG. 2. Molecular model of Fas-FasL interaction.** Ribbon representation of the Fas-FasL hexameric complex. The ligand monomers are depicted in blue, while the receptor molecules are shown in light green and disulfide bridges in yellow. The pink structures represent the volume occupied by the nine *N*-linked glycans attached to Asn-184, Asn-250, and Asn-260. *N*, Asn. A, top view of the complex; B, side view of a simplified representation showing only subunit A of the Fas ligand and its two bound receptor molecules. Transmembrane domains of Fas and FasL would be at the top and at the bottom of the figure, respectively.

was further refined by 200 cycles of energy minimization with CHARMM (53). The three *N*-glycosylation sites are located at Asn-184, Asn-250, and Asn-260 in the FasL model. A short branched *N*-linked glycan structure (GlcNAc $\beta$ 1-4Man $\alpha$ 1-6[Man $\alpha$ 1-3]Man $\beta$ 1-4GlcNAc $\beta$ 1-4GlcNAc) was extracted from Brookhaven Protein Data Bank entry 9API, and was linked to the respective asparagines using interactive graphics.

## RESULTS AND DISCUSSION

**Glycosylation of sFasL**—A plasmid encoding the signal peptide of hemagglutinin, in frame with a flag epitope and the COOH-terminal portion of the extracellular domain of human Fas ligand (amino acids 139–281), was transfected into the human embryonic kidney 293 cell line. Secreted sFasL was affinity-purified using immobilized anti-flag antibodies. The

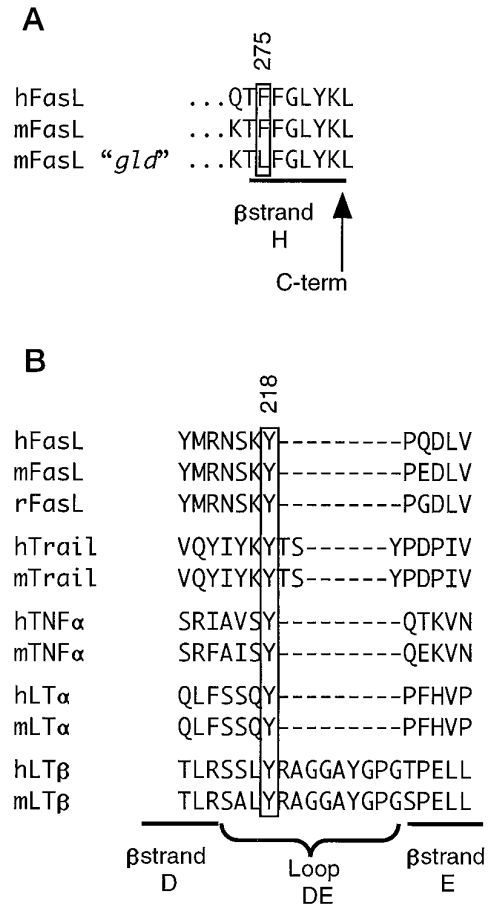


**FIG. 3. Sequence alignment of the COOH terminus of FasL and of the loop DE region of TNF family members.** Panel A, carboxyl-terminal sequence of human and murine FasL showing the site of the *gld* mutation (box). Numbering refers to the human FasL sequence. Panel B, sequence alignment of various ligands around loop DE. The conserved Tyr residue is boxed (position 218 in human FasL). Note that this Tyr residue is not conserved in CD27L, CD30L, and CD40L.

theoretical molecular mass of the encoded recombinant protein is 18.2 kDa. Purified sFasL migrated as a doublet on SDS-PAGE with deduced molecular masses of 29 and 25.5 kDa (Fig. 1A). Taken together with previous data (55), this heterogeneity and the discrepancy between predicted and observed molecular masses suggest that carbohydrates are present on the sFasL. Indeed, sFasL present in both cell extracts and cell supernatants could be digested with peptide *N*-glycanase F to a single band with the predicted molecular mass of 18 kDa (Fig. 1B), indicating that the various species of sFasL differed by their degree of *N*-glycosylation. This result was confirmed when cells were treated with the *N*-glycosylation inhibitor tunicamycin; a dose-dependent accumulation of cellular, unglycosylated 18-kDa sFasL was observed with concomitant loss of sFasL secretion (Fig. 1C). A total of four evenly spaced bands of sFasL could be detected, which probably correspond to the unglycosylated, mono-, di-, and tri-*N*-glycosylated sFasL monomers. Thus, all three potential *N*-glycosylation sites of human FasL (Asn-184, Asn-250, and Asn-260) appear to be used. Interestingly, secreted sFasL is consistently found in its highly glycosylated form, even at intermediate tunicamycin concentrations where unglycosylated sFasL is by far the predominant cellular species (Fig. 1C). This strongly suggests that *N*-linked oligosaccharides are required for efficient secretion of sFasL.

We next generated a molecular model of the FasL-Fas complex (Fig. 2) using knowledge-based protein modeling methods and the known tridimensional structures of lymphotoxin  $\alpha$

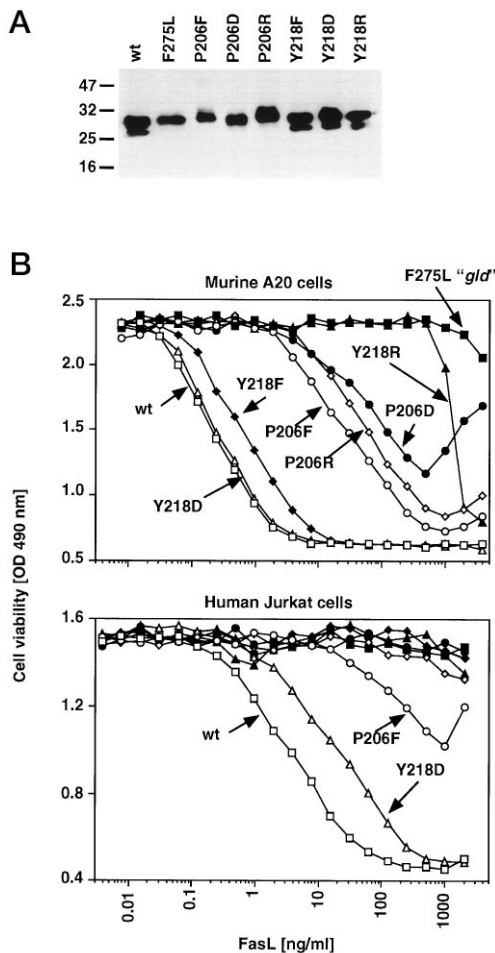


**FIG. 4. Expression and cytotoxic activity of wild type and mutant sFasL.** *Panel A*, Western blot of concentrated supernatant from transiently transfected 293T cells as detected by antibody staining with the anti-flag M2 antibody. Ten-fold more supernatant of mutant F275L was loaded to achieve a similar intensity of staining. *wt*, wild type. *Panel B*, cytotoxic activity of sFasL mutants on murine and human cells. Murine A20 cells (*upper graphs*) and human Jurkat cells (*bottom graphs*) were incubated at 37 °C in the presence of the indicated concentrations of wild type or mutant sFasL, and of 1  $\mu$ g/ml M2 antibody. After 8 h, the phenazine methosulfate/MTS reagent was added, and the incubation was carried out for an additional 4 h. The cell viability was monitored at 490 nm. *Open squares*, wild type sFasL (*wt*); *closed squares*, F275L; *open circles*, P206F; *closed circles*, P206D; *open diamonds*, P206R; *closed diamonds*, Y218F; *open triangles*, Y218D; *closed triangles*, Y218R.

(TNF $\beta$ ) and the 55-kDa tumor necrosis factor receptor (49). It can be seen that the *N*-linked oligosaccharides are concentrated on the lateral edge of each FasL monomer, leaving vertical clefts, which would allow the receptor to reach the interaction site of the ligand.

Two of the three glycosylation sites of the FasL have counterparts in other family members. Residue Asn-260 of FasL is also found at the corresponding position in lymphotoxin  $\beta$ , CD27L, and CD40L, whereas residue Asn-250 of FasL corresponds to a site in CD30L. In some TNF family members, *N*-glycosylation appears to be important for the biological activity of the protein. For example, FasL, which can be expressed in a variety of eukaryotic systems (20, 56, 57), forms inactive inclusion bodies when expressed in bacteria.<sup>2</sup> The extensively glycosylated CD30L (four putative *N*-glycosylation sites) is also best produced in a recombinant form in eukaryotic systems (57). Glycosylated recombinant CD40L is readily ex-

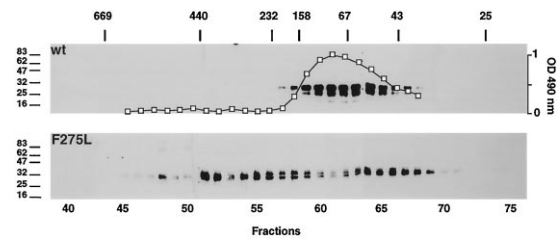


**FIG. 5. Size exclusion chromatography of sFasL on Superdex-200.** Concentrated supernatants containing wild type or F275L "gld" sFasL were fractionated on a Superdex-200 column. Eluted fractions were analyzed by Western blotting and the sFasL detected with M2 antibody. The migration positions of the molecular mass markers (in kDa) are indicated on the *left hand side* for SDS-PAGE and at the *top* of the figure for size exclusion chromatography. The graph superimposed on the wild type elution profile (*wt*) represents the signal obtained for 5  $\mu$ l of each fraction in a hFas-Fc/FasL interaction ELISA, as described in the legend to Fig. 7.

pressed at the surface of eukaryotic cells, but transport to the cell surface is blocked in the presence of the *N*-glycosylation inhibitor tunicamycin (57). In contrast, TNF $\alpha$  (58) and lymphotoxin  $\alpha$  (59) can be produced in a soluble, non-glycosylated and active form in prokaryotic expression systems. When these two latter ligands are expressed in eukaryotic systems, *N*-glycosylation can result in minor effects such as a 10-fold decrease in specific activity of TNF $\alpha$  (60) or the masking of epitopes recognized by neutralizing antibodies for lymphotoxin  $\alpha$  (61). This supports the conclusion that *N*-glycosylation can be important for the efficient secretion of FasL and other glycosylated ligands of this family.

*The Mouse gld Mutation Also Renders Human sFasL Inactive*—The availability of an efficient system for the production of recombinant sFasL allowed us to test the validity of the structural model of the Fas-FasL by generating a number of mutants (Fig. 3). A well characterized spontaneous mutation (F273L) in murine FasL, called *gld*, abolishes FasL activity and results in a phenotype of generalized lymphoproliferative disease (15). The mutant F275L was engineered to test whether an analogous mutation would also inactivate human FasL (Fig. 3A). The yield of F275L sFasL secretion was low compared with wild type sFasL, but its molecular weight suggested that it was completely *N*-glycosylated (Fig. 4A, *lane F275L*). The F275L mutation had a severe effect on the cytotoxic activity of sFasL, which was reduced by more than 5 orders of magnitude compared with wild type (Fig. 4B). These results raised the question of whether the F275L mutant was properly folded and trimerized. Therefore wild type and mutated FasL were analyzed by gel permeation chromatography. Wild type FasL eluted as a defined peak with an apparent molecular mass of 79 kDa (corresponding to a 2.7-mer), whereas the F275L mutant eluted broadly throughout the profile (Fig. 5). It is conceivable that this mutation, occurring at the hydrophobic interface of two monomers (62), prevents correct association of otherwise properly folded monomers leading to uncontrolled association and impairment of binding to Fas. Interestingly, FasL is normally expressed at the surface of activated T-lymphocytes from *gld* mice (62), raising the question of whether the structural impact of the *gld* mutation is less severe in the murine protein as compared with human FasL.

*Amino Acid Residues Pro-206 and Tyr-218 of FasL Are Important for the Interaction with Fas*—Due to their predicted close proximity to the receptor (Fig. 6), amino acids Pro-206 and Tyr-218 were chosen for mutagenesis. The mutants P206F, P206D, and P206R were secreted and glycosylated (Fig. 4A), and were between 100-fold (for P206F) and 500-fold (for P206D) less active than wild type FasL (Fig. 4B). The binding of the FasL to Fas was determined *in vitro* with a Fas-FasL

<sup>2</sup> P. Schneider, unpublished observation.

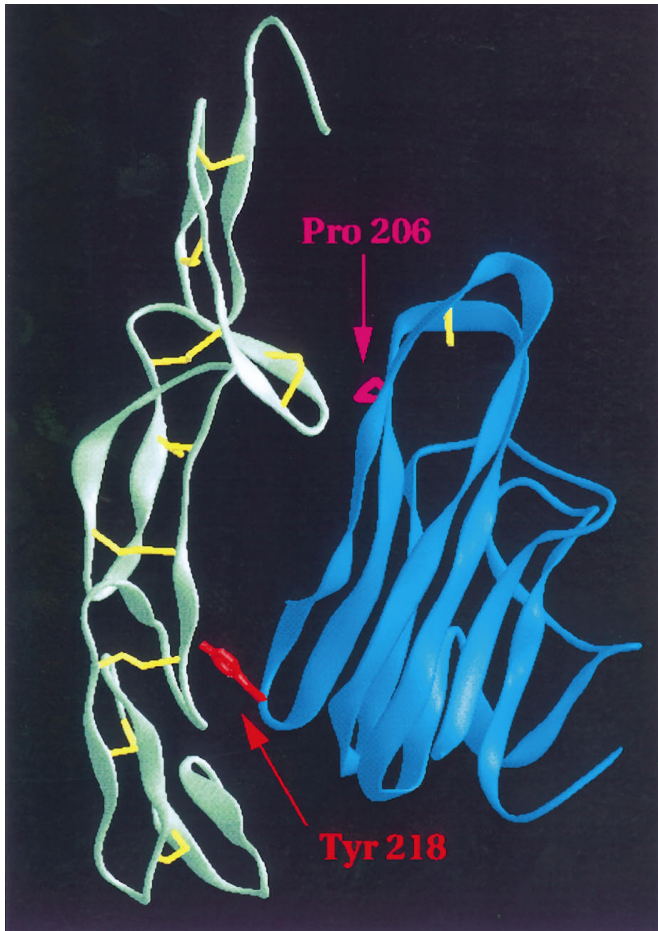


FIG. 6. Location of Pro-206 and Tyr-218 of FasL in the structural model of Fas-FasL. A single ligand subunit and a single receptor are shown.

interaction ELISA. In this assay, recombinant FasL is captured by chimeric Fas-Fc coated on plastic, and the interaction is detected by antibody binding to the flag epitope present at the NH<sub>2</sub> terminus of the sFasL (Fig. 7). The binding affinity was strong for wild type FasL, weak yet significant for the Pro-206 mutants, and equal to background for the F275L “gld” mutant, correlating with their respective potency to induce apoptosis in target cells. These results suggest that the Pro-206 residue of the FasL is directly involved in the Fas-FasL interaction, although we cannot formally exclude that the observed phenotype is the result of the structural impact of the mutation on FasL.

Tyr-218 is located in a loop between  $\beta$ -strands D and E of the FasL (Figs. 3B and 6). This residue is conserved among a number of ligands, including all known death-inducing ligands (Fig. 3B). This is a remarkable feature, as loop residues are normally highly variable between family members. Moreover, this tyrosine residue is known to be essential for lymphotoxin  $\alpha$  (TNF $\beta$ ) and TNF $\alpha$  binding to TNF-receptor I (49, 59, 63).

Surprisingly, the Y218D mutant and the wild type FasL have similar abilities to kill both murine and human target cells (Fig. 4B) and to bind to recombinant Fas of both species (Fig. 7B). This is, however, in sharp contrast with the Y218R mutant, which is 4 orders of magnitude less active than wild type FasL on murine cells, and which displays impaired binding to Fas (Figs. 4B and 7B). This latter mutant is, however, very similar to wild type FasL by other criteria such as secretion efficiency, glycosylation, and size as determined by gel permeation chromatography (Fig. 4A and data not shown). The

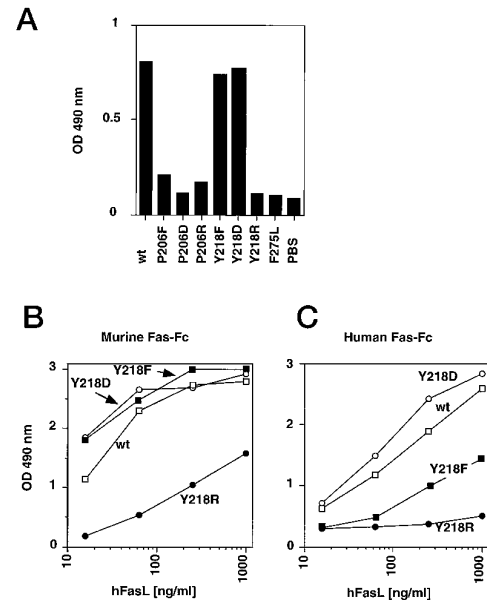


FIG. 7. Fas-FasL interaction measured by ELISA. The extracellular domains of murine (panels A and B) or human (panel C) Fas fused to the Fc portion of a human IgG1 were coated on immunoplates and used to capture wild type (*wt*) or mutant human sFasL. Bound sFasL was detected using the M2 antibody and an anti-mouse peroxidase conjugate. In panel A, wild type and mutated sFasL were used at a single concentration of 200 ng/ml. In panels B and C, selected sFasL (wild type and the Tyr-218 mutants) were used at the indicated concentrations.

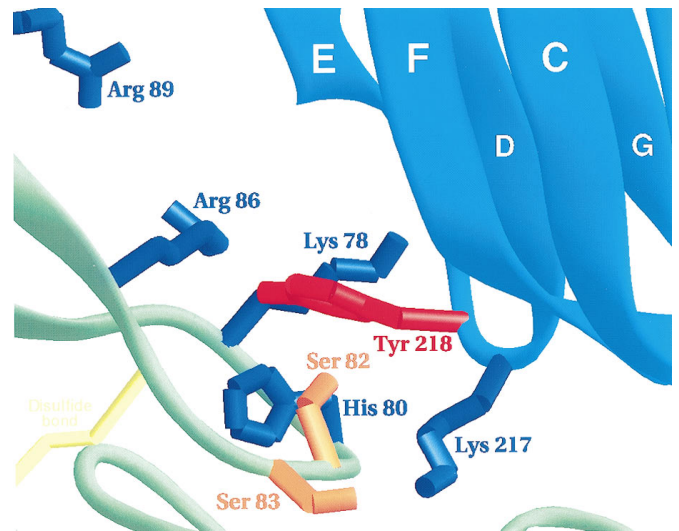


FIG. 8. Molecular model of the Fas-FasL contact site in the area of FasL Tyr-218. The ligand monomer is depicted in light green, while the receptor molecule is shown in light yellow. Tyr-218 of FasL, which was mutated to Phe, Asp, and Arg, is represented in red, while residues bearing a positive charge and histidine are shown in blue. Ser-83 of hFas is an Asp-74 residue in muFas.

region of Fas interacting with Tyr-218 is rich in basic amino acid residues (Fig. 8). The phenol group of the tyrosine is therefore likely to form hydrogen bonds with Fas, and could even exist as phenolate in this environment to form a salt bridge with Fas. In this context, changing the Tyr residue for a negatively charged Asp residue can be considered as a conservative mutation. In contrast, mutation of the Tyr residue for a positively charged Arg residue (Y218R) will not only disrupt the existing interactions but will add a detrimental electrostatic repulsion leading to the observed greatly impaired cytotoxic phenotype.

TABLE I

Residues of Fas predicted to be involved in Fas-FasL interaction and differing between human and murine FasL

Each Fas receptor molecule interacts with two FasL subunits. Thus, each residue in the protein-protein contact area can interact with either a subunit on the left hand side (L), on the right hand side (R), or on both sides (LR).

No.	Human	Murine	Subunit
1	Phe-81	Tyr-72	L
2	Ser-82	Ala-73	L
3	Ser-83	Asp-74	LR
4	Arg-89	Thr-80	R
5	Gly-94	Glu-85	R
6	Thr-122	Pro-113	L
7	Val-123	Gly-114	L

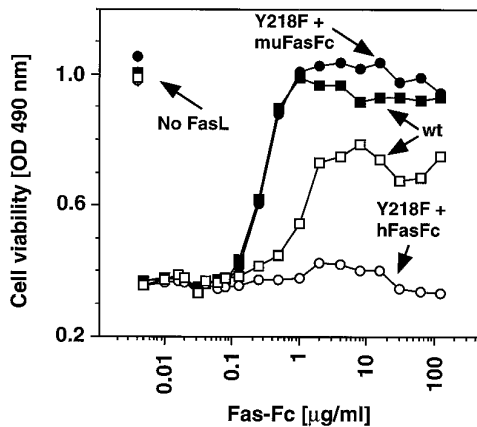


FIG. 9. **Species specificity of sFasL Y218F.** Murine A20 cells were incubated for 4 h with a lethal dose (30 ng/ml) of either wild type (squares) or Y218F (circles) sFasL, and in the presence of increasing amounts of either hFas-Fc (open symbols) or muFas-Fc (closed symbols) fusion proteins as described under "Experimental Procedures." Cell viability was monitored as described in the legend to Fig. 4. The signal obtained in the absence of sFasL (open square) is indicated by an arrow.

It has been shown recently that the amino acid residue Arg-86 (but not Lys-78) of Fas is essential for ligand binding (64). Taken together with our results, this suggests that a strong interaction takes place between Tyr-218 of FasL and Arg-86 of Fas (Fig. 8).

**The Y218F sFasL Mutant Specifically Interacts with Murine but Not Human Fas**—The effect of the Y218F mutation on sFasL should be intermediate between that seen for the Y218D and Y218R mutations described above, since the positive interaction of the phenol group of Tyr-218 with Fas should be lost without generating additional repulsion. As expected from this model, the Y218F mutant of FasL displays intermediate cytotoxic activity (Fig. 4B). Interestingly, the cytotoxic effect of this mutant is markedly dependent upon the species from which the receptor derives, which is in contrast with the documented complete cross-reactivity between wild type human and murine FasL and Fas (38). The Y218F mutant is relatively potent at killing murine target cells and is apparently inactive on human target cells (Fig. 4B). This species specificity is also evident at the level of recombinant Fas binding (Fig. 7). This suggests that the binding of the sFasL to murine Fas relies on more frequent, or more stable interactions than to human Fas. Destroying the Tyr-218 interaction site is therefore less detrimental for murine Fas binding activity than for human Fas. A list of Fas residues, which are likely to be involved in FasL binding but which are different between both species, is given in Table I. This difference in activity between murine and human Fas was not due to the presence of an Asp-74 in murine Fas instead of a Ser-83 in human Fas (Table I and data not shown). Similar

effects of specificity restriction have been observed in TNF $\alpha$ , where point mutations induced marked specificity for either TNF-R1 or TNF-R2 (58).

If the Y218F sFasL mutant is species-specific, it should be able to exert its cytotoxic effect on murine target cells even in the presence of an excess of soluble recombinant human Fas, but should be inhibited by recombinant murine Fas. In contrast, wild type sFasL should be inhibited by recombinant Fas from both species. To confirm this point, murine target cells were exposed to a lethal dose of either wild type or Y218F sFasL, in the presence of increasing amounts of recombinant human or murine Fas-Fc fusion proteins (Fig. 9). As predicted, Y218F sFasL was inhibited by murine Fas-Fc but left practically unaffected by human Fas-Fc. In contrast, wild type sFasL was inhibited by both fusion proteins (Fig. 9). This experiment demonstrates the strong (however not absolute) species specificity of Y218F sFasL toward murine Fas.

In summary, we have found that the *N*-glycosylation of sFasL is required for its solubility, and we describe a method for its production and purification. The availability of sFasL (and its inhibitor Fas-Fc) will prove useful to study a variety of systems in which Fas and FasL are implicated. In addition, the model that we presented here allowed us to successfully design mutations affecting the binding of FasL to Fas, and should therefore facilitate the design of specific inhibitors of Fas-FasL inhibitors.

**Acknowledgments**—We are grateful to Dr. D. Rimoldi for providing us with human activated PBL cDNA and to S. Belli for careful reading of the manuscript.

## REFERENCES

- Nagata, S. (1997) *Cell* **88**, 355–365
- Smith, C. A., Farrar, T., and Goodwin, R. G. (1994) *Cell* **76**, 959–962
- Kägi, D., Vignaux, F., Lerdemann, B., Bürki, K., Deraetere, V., Nagata, S., Hengartner, H., and Goldstein, P. (1994) *Science* **265**, 528–530
- Lowin, B., Hahne, M., Mattmann, C., and Tschopp, J. (1994) *Nature* **370**, 650–652
- Tsutsui, H., Nakanishi, K., Matsui, K., Higashino, K., Okamura, H., Miyazawa, Y., and Kaneda, K. (1996) *J. Immunol.* **157**, 3967–3973
- Rathmell, J. C., Cooke, M. P., Ho, W. Y., Grein, J., Townsend, S. E., Davis, M. M., and Goodnow, C. C. (1995) *Nature* **376**, 181–184
- Alderson, M. R., Tough, T. W., Davis-Smith, T., Braddy, S., Falk, B., Schooley, K. A., Goodwin, R. G., Smith, C. A., Ramsdell, F., and Lynch, D. H. (1995) *J. Exp. Med.* **181**, 71–77
- Brunner, T., Mogil, R. J., LaFace, D., Yoo, N. J., Mahboubi, A., Echeverri, F., Martin, S. J., Force, W. R., Lynch, D. H., Ware, C. F., and Green, D. R. (1995) *Nature* **373**, 441–444
- Dhein, J., Walczak, H., Baumler, C., Debatin, K.-M., and Krammer, P. H. (1995) *Nature* **373**, 438–441
- Ju, S.-T., Panka, D. J., Cui, H., Ettinger, R., El-Khatib, M., Sherr, D. H., Stanger, B. Z., and Marshak-Rothstein, A. (1995) *Nature* **373**, 444–448
- Griffith, T., Brunner, T., Fletcher, S., Green, D., and Ferguson, T. (1995) *Science* **270**, 1189–1192
- Bellgrau, D., Gold, D., Selawry, H., Moore, J., Franzusoff, A., and Duke, R. C. (1995) *Nature* **377**, 630–632
- Lau, H. T., Yu, M., Fontana, A., and Stoeckert, C. J. (1996) *Science* **273**, 109–112
- Watanabe-Fukunaga, R., Brannan, C. I., Copeland, N. G., Jenkins, N. A., and Nagata, S. (1992) *Nature* **356**, 314–317
- Takahashi, T., Tanaka, M., Brannan, C. I., Jenkins, N. A., Copeland, N. G., Suda, T., and Nagata, S. (1994) *Cell* **76**, 969–976
- Fisher, G. H., Rosenberg, F. J., Straus, S. E., Dale, J. K., Middleton, L. A., Lin, A. Y., Strober, W., Lenardo, M. J., and Puck, J. M. (1995) *Cell* **81**, 935–946
- Rieux-Laucat, F., Le Deist, F., Hivroz, C., Roberts, I. A. G., Debatin, K. M., Fisher, A., and de Villartay, J. P. (1995) *Science* **268**, 1347–1349
- Wu, J., Wilson, J., He, J., Xiang, L. B., Schur, P. H., Mountz, J. D. (1996) *J. Clinical. Invest.* **98**, 1107–1113
- Adachi, M., Suematsu, S., Suda, T., Watanabe, D., Fukuyama, H., Ogasawara, J., Tanaka, T., Yoshida, N., and Nagata, S. (1996) *Proc. Natl. Acad. Sci. U. S. A.* **93**, 2131–2136
- Tanaka, M., Suda, T., Haze, K., Nakamura, N., Sato, K., Kimura, F., Motoyoshi, K., Mizuki, M., Tagawa, S., Ohga, S., Hatake, K., Drummond, A. H., and Nagata, S. (1996) *Nat. Med.* **2**, 317–322
- Sato, K., Kimura, F., Nakamura, Y., Murakami, H., Yoshida, M., Tanaka, M., Nagata, S., Kanatani, Y., Wakimoto, N., Nagata, N., and Motoyoshi, K. (1996) *Br. J. Haematol.* **94**, 379–382
- O'Connell, J., O'Sullivan, G. C., Collins, J. K., and Shanahan, F. (1996) *J. Exp. Med.* **184**, 1075–1082
- Strand, S., Hofmann, W. J., Hug, H., Muller, M., Otto, G., Strand, D., Mariani, S. M., Stremmel, W., Krammer, P. H., and Galle, P. R. (1996) *Nat. Med.* **2**, 1361–1366

24. Hahne, M., Rimoldi, D., Schröter, M., Romero, P., Schreier, M., French, L. E., Schneider, P., Bornand, T., Fontana, A., Lienard, D., Cerottini, J.-C., and Tschopp, J. (1996) *Science* **274**, 1363–1366
25. Westendorp, M. O., Frank, R., Ochsenbauer, C., Stricker, K., Dhein, J., Walczak, H., Debatin, K.-M. and Krammer, P. H. (1995) *Nature* **375**, 497–500
26. Katsikis, P. D., Wunderlich, E. S., Smith, C. A., Herzenberg, L. A., and Herzenberg, L. A. (1995) *J. Exp. Med.* **181**, 2029–2036
27. Estaquier, J., Tanaka, M., Suda, T., Nagata, S., Golstein, P., and Ameisen, J. C. (1996) *Blood* **87**, 4959–4966
28. Dowling, P., Shang, G. F., Raval, S., Menonna, J., Cook, S., and Husar, W. (1996) *J. Exp. Med.* **184**, 1513–1518
29. Via, C. S., Nguyen, P., Shustov, A., Drappa, J., and Elkon, K. B. (1996) *J. Immunol.* **157**, 5387–5393
30. Braun, M. Y., Lowin, B., French, L., Acha-Orbea, H., and Tschopp, J. (1996) *J. Exp. Med.* **183**, 657–661
31. Gearing, A. J. H., Beckett, P., Christodoulou, M., Churchill, M., Clements, J., Davidson, A. H., Drummond, A. H., Galloway, W. A., Gilbert, R., Gordon, J. L., Leber, T. M., Mangan, M., Miller, K., Nayee, P., Owen, K., Patel, S., Thomas, W., Wells, G., Wood, L. M., and Woolley, K. (1994) *Nature* **370**, 555–557
32. Kayagaki, N., Kawasaki, A., Ebata, T., Ohmoto, H., Ikeda, S., Inoue, S., Yoshino, K., Okumura, K., and Yagita, H. (1995) *J. Exp. Med.* **182**, 1777–1783
33. Mariani, S. M., Matiba, B., Bäumlner, C., and Krammer, P. H. (1995) *Eur. J. Immunol.* **25**, 2303–2307
34. Martinez-Lorenzo, M. J., Alava, M. A., Anel, A., Piñeiro, A., and Naval, J. (1996) *Immunology* **89**, 511–517
35. Jones, E. Y., Stuart, D. I., and Walker, N. P. C. (1989) *Nature* **338**, 225–228
36. Eck, M. J., Ultsch, M., Rinderknecht, E., de Vos, A. M., and Sprang, S. R. (1992) *J. Biol. Chem.* **267**, 2119–2122
37. Karpusas, M., Hsu, Y.-M., Wang, J.-H., Thompson, J., Lederman, S., Chess, L., and Thomas, D. (1995) *Structure* **3**, 1031–1039
38. Takahashi, T., Tanaka, M., Inazawa, J., Abe, T., Suda, T., and Nagata, S. (1994) *Int. Immunol.* **6**, 1567–1574
39. Wiley, S. R., Schooley, K., Smolak, P. J., Din, W. S., Huang, C.-P., Nicholl, J. K., Sutherland, G. R., Smith, T. D., Rauch, C., Smith, C. A., and Goodwin, R. G. (1995) *Immunity* **3**, 673–682
40. Gething, M.-J., Bye, J., Skehel, J., and Waterfield, M. (1980) *Nature* **287**, 301–306
41. Hopp, T. P., Prickett, K. S., Price, V. L., Liggy, R. T., March, C. J., Cerreti, D. P., Urdal, D. L., and Conlon, P. J. (1988) *Biotechnology* **6**, 1204–1210
42. Peppel, K., Crawford, D., and Beutler, B. (1991) *J. Exp. Med.* **174**, 1483–1489
43. Kingston, R. E. (1995) in *Current Protocols in Molecular Biology* (Ausubel, F. M., Brent, R., Kingston, R. E., Moore, D. D., Seidman, J. G., Smith, J. A., and Struhl, K., eds) pp. 9.1.1–9.1.11, John Wiley & Sons, New York
44. Laemmli, U. K. (1970) *Nature* **227**, 680–685
45. Towbin, H., Staehelin, T., and Gordon, J. (1979) *Proc. Natl. Acad. Sci. U. S. A.* **76**, 4350–4354
46. Peitsch, M. C. (1995) *Biotechnology* **13**, 658–660
47. Peitsch, M. C. (1996) *Biochem. Soc. Trans.* **24**, 274–279
48. Eck, M. J., and Sprang, S. R. (1989) *J. Biol. Chem.* **264**, 17595–17605
49. Banner, D. W., D'Arcy, A., Janes, W., Gentz, R., Schoenfeld, H.-J., Broger, C., Loetscher, H., and Lesslauer, W. (1993) *Cell* **73**, 431–445
50. Peitsch, M. C., and Tschopp, J. (1995) *Mol. Immunol.* **32**, 761–772
51. Peitsch, M. C., and Jongeneel, C. V. (1993) *Int. Immunol.* **5**, 233–238
52. Luethy, R., Bowie, J. U., and Eisenberg, D. (1992) *Nature* **356**, 83–85
53. Sippl, M. J. (1993) *Proteins* **17**, 355–362
54. Brooks, B. R., Bruccoleri, R. E., Olafson, B. D., States, D. J., Swaminathan, S., and Karplus, M. (1983) *J. Comput. Chem.* **4**, 187–217
55. Tanaka, M., Suda, T., Takahashi, T., and Nagata, S. (1995) *EMBO J.* **14**, 1129–1135
56. Mariani, S. M., Matiba, B., Sparna, T., and Krammer, P. H. (1996) *J. Immunol. Methods* **193**, 63–70
57. Jumper, M. D., Nishioka, Y., Davis, L. S., Lipsky, P. E., and Meek, K. (1995) *J. Immunol.* **155**, 2369–2378
58. Van Ostade, X., Vandenaabeele, P., Tavernier, J., and Fiers, W. (1994) *Eur. J. Biochem.* **220**, 771–779
59. Goh, C. R., Loh, C.-S., and Porter, A. G. (1991) *Protein Eng.* **4**, 785–792
60. Koyama, Y., Hayashi, T., Fujii, N., and Yoshida, T. (1992) *Biochim. Biophys. Acta* **1132**, 188–194
61. Benjamin, D., Kofler, G., and Tschachler, E. (1992) *Lymphokine Cytokine Res.* **11**, 45–54
62. Hahne, M., Peitsch, M. C., Irmeler, M., Schröter, M., Lowin, B., Rousseau, M., Bron, C., Renno, T., French, L., and Tschopp, J. (1995) *Int. Immunol.* **7**, 1381–1386
63. Zhang, X.-M., Weber, I., and Chen, M.-J. (1992) *J. Biol. Chem.* **267**, 24069–24075
64. Starling, G. C., Bajorath, J., Emswiler, J., Ledbetter, J. A., Aruffo, A., and Kiener, P. A. (1997) *J. Exp. Med.* **185**, 1487–1492